Hindawi
Advances in Materials Science and Engineering
Volume 2022, Article ID 3054214, 8 pages
https://doi.org/10.1155/2022/3054214

*Research Article*

# Thermal and Waterproof Properties of Foamed Concrete with Nano $SiO_2$ Aerogel and Organosilicon Waterproofing Agent

**Baojun Cheng,[1,2] Xiaowei Gu,[1] Yuxin Gao,[2,3] Pengfei Ma,[2,3] and Shengrong Kang[2]**

[1]*Northeastern University, Shenyang 110819, China*
[2]*China Construction West Building Materials Science Research Institute Co. Ltd, Chengdu 610094, China*
[3]*Chongqing University, Chongqing 400044, China*

Correspondence should be addressed to Xiaowei Gu; xiaoweigu@outlook.com

Received 11 August 2021; Revised 9 March 2022; Accepted 1 April 2022; Published 10 May 2022

Academic Editor: Robert Černý



This paper aimed to improve the thermal and waterproof properties of foamed concrete through the synergic work of nano $SiO_2$ aerogel powder (NSAP) and organosilicon waterproofing agent (OWA). Hence, several series of foamed concrete with a 0–3.0% of OWA and with 1–4% of NSAP addition were developed. The results show that OWA can decrease the dry bulk density, compressive strength, water absorption rate, and thermal conductivity. With the addition of NSAP, the water absorption rate reached a minimum value of 9.2% at 3.0% NSAP, while the thermal conductivity continued decreasing. Through the microscopic pore size distribution, XRD, and SEM, it was found that the addition of NSAP had no effect on the type of hydration product, but it can increase the average pore size and the amount of macropore and weaken the interfacial adhesion between hydration products. Comparing the heat transmission model, the presence of NSAP increased the heat transmission pathway and resistance, resulting in lower thermal conductivity.

## 1. Introduction

Foamed concrete is a lightweight porous material prepared by introducing premanufactured aqueous foam into the cement or mortar paste [1], with light weight, good thermal insulation and sound insulation performance, fire resistance, low cost, and recycling waste [2, 3]. However, the foamed concretes generally show a poor thermal conductivity, low mechanical strength, and high water absorption rate, which greatly restricts its application in construction industries; thus, a low-density foamed concrete with excellent properties is difficult to prepare [4, 5]. As foamed concrete or other porous materials are easily damaged by water hydrolysis, it can be blended with nanoaerogel or nanomaterials to solve the problem [6–8].

Kistler discovered aerogels 80 years ago [9] by complex synthesis in supercritical drying conditions. Depending on the silica source and the preparation process, aerogels have significant physical, thermal, optical, and acoustic properties [10]. To overcome the problems of foamed concrete, some experiments [11, 12] were attempted to enhance the thermal transfer and moisture resistances of foamed concrete by merging with aerogel technologies. The thermal conductivity of foam concrete with hydrophobic aerogel is 0.08 W/m·K approximately, which corresponds to be 30–50% for conventional foam concrete [13]. And the waterproof capacity of foam concrete with hydrophobic aerogel was significantly improved, resulting in exhibiting 75% lower water absorption at an age of 24 hours when compared with the conventional foam concrete [13].

Nano $SiO_2$ aerogel is a porous and solid material with the lowest thermal conductivity and density. It is widely used in heat insulation, aerospace, environmental protection, new energy, and other fields [14]. In recent years, it has been found that adding nano $SiO_2$ aerogel powder (NSAP) into the foamed concrete can effectively reduce the bulk density and thermal conductivity of foamed concrete [15]. The aerogel foamed concrete (AFC) presented a lower thermal conductivity and bulk density than normal foamed concrete. However, the waterproofing properties of AFC have not

been significantly improved with the addition of NSAP, which can damage its thermal insulation performance when the AFC was contacted with water or in a humid environment. Moreover, when the AFC was used in cold or severe cold areas, the strength was hugely reduced due to the alternate freezing and thawing cycles [16], resulting in the damage of the foamed concrete structure.

From the literature, it was concluded that the addition of supplementary cementitious materials and fibers could significantly improve the mechanical properties. The waterproofing agents can improve the water resistance, and the NSAP can reduce its bulk density. However, the addition of NSAP fillers simultaneously with waterproofing agents in foamed concrete to reduce their thermal conductivity and improve their water resistance has not been engaging in the literature, which restricts its application in the construction industry. Therefore, more attention should be paid to determine the synergic work between NSAP and waterproof materials on the thermal insulation performance and water resistance of foamed concrete. In this study, the influence of NSAP and organosilicon waterproofing agents on the thermal and waterproofing properties of AFC was studied.

## 2. Experimental Studies

*2.1. Materials.* The ordinary Portland cement (PC) used in this study was P·O 42.5R conforming to the Chinese Standard for ordinary Portland cement. The fly ash (FA) used in this study was grade Ⅰ FA, which conforms to the Chinese Standard for fly ash used for cement and concrete. The physical and chemical properties of PC and FA are given in Table 1. The density of PC and FA is 3080 kg/m$^3$ and 2340 kg/m$^3$, respectively. NSAP is white and translucent produced by Suzhou Rexiang Nano Technology Co., Ltd., with an average particle size of 15 um, a thermal conductivity of 0.015 W/(m·K) (25°C), and a density of 0.08 g/cm$^3$. Foaming agent is HTQ-1 compound foaming agent produced by Henan Huatai New Material Technology Co., Ltd. The accelerator is a self-made composite accelerator, and hydroxypropylmethylcellulose (HPMC) is from Shandong Gomez Chemical Co., Ltd. The water reducing agent is polycarboxylic acid superplasticizer (SP) with a water reducing rate of 35% and a solid content of 50%. Organosilicon waterproofing agent (OWA) was from Wacker Chemical Co., Ltd.

*2.2. Preparation of Specimens.* First, the specimens with OWA at 0%, 0.1%, 0.5%, 1.0%, and 3.0% of the scale specimens were studied. Then, the specimens with OWA at 0.5% while NSAP ranging from 1.0% to 4.0% were also studied. The wet density of all AFC pastes was controlled from 280 kg/m3 to 300 kg/m$^3$. The mix designs of AFC are shown in Table 2. In order to ensure good performance of aerogel foam concrete, 10wt% fly ash is added in the mixture.

*2.3. Mixing Procedure.* The mixing procedures of AFC were as follows. Firstly, the PC, FA, HPMC, accelerator, OWA, and NSAP, according to the mix proportions in Table 2, were uniformly dry-mixed for 2-3 min. Then, the tap water and SP were added to the premixed powders and mixed for 3 min. Finally, the preformed foam was added to the paste and mixed for 3 min. Additionally, the following specimens were cast to determine the mechanical properties: the cubic specimens $100 \times 100 \times 100\,mm^3$ for testing the compressive strength and the dry bulk density. In addition, prismatic specimen $300 \times 300 \times 30\,mm^3$ was used to test the thermal conductivity. All the specimens were cast into molds and covered with cling film to prevent water evaporation. After 72 h, the specimens were demolded and kept in a standard curing room (20°C, 100% relative humidity) for 28 days. Before tests, each specimen was dried in an oven at 60°C to a constant weight and cooled to room temperature.

Table 1: The chemical composition of cementitious materials (wt%).

| Chemical composition | PC | FA |
|---|---|---|
| $SiO_2$ | 21.39 | 50.39 |
| $Al_2O_3$ | 5.15 | 27.49 |
| CaO | 61.04 | 4.47 |
| MgO | 2.82 | 0.953 |
| $Na_2O$ | 0.638 | 1.41 |
| $K_2O$ | 0.615 | 2.03 |
| $P_2O_5$ | 0.095 | 0.357 |
| $Fe_2O_3$ | 3.86 | 8.47 |
| $TiO_2$ | 0.848 | 2.92 |
| $SO_3$ | 3.10 | 1.16 |
| Others | 0.444 | 0.35 |

*2.4. Test Procedures.* The 28 days compressive strength of the AFC was determined by a sensitive multifunctional testing system machine with a 200 KN capacity. The bulk density of the AFC was calculated by dividing the dry mass of the AFC to its volume ($100 \times 100 \times 100\,mm^3$) at the age of 28 days. The water absorption rate was calculated based on the difference in the mass before and after immersion in water for 24 h. The thermal conductivity ($k$) of AFC was measured in accordance with ASTM C518 Standard Test Method for Steady-State Thermal Transmission Properties by means of the Heat Flow Meter Apparatus on HFM 436 by NETZSCH.

The pore structure of the AFC was measured by the specimen of 100 mm × 100 mm × 100 mm cut in half, and the section was the surface to be measured. DJCK-2 crack width meter manufactured by Jingmao Instrument was used to photograph the structure of the cut face. The size of the section was 11 × 9 mm, and the magnification was 60 times. Finally, Namo Measurer software was used for statistical analysis of pore structure parameters.

The micromorphology of AFC was observed by scanning electron microscope (SEM). Due to the poor conductivity of the sample, the sample was sprayed with gold before testing. The phase composition of AFC was analyzed by Powder X-ray Diffraction analyzer (XRD, Shimadzu DX-6100).

## 3. Results and Discussion

*3.1. Influence of OWA Content on Fundamental Properties.* The fundamental properties of the AFC with different OWA contents are presented in Figure 1. It was observed that with

Table 2: The mix designs of AFC (kg/m$^3$).

| Mix | PC | FA | Water | SP | HPMC | Accelerator | OWA (wt%) | NSAP (wt%) |
|---|---|---|---|---|---|---|---|---|
| AFC-0 | 225 | 25 | 62.5 | 1.5 | 0.075 | 30 | 0 | 0 |
| AFC-1 | 225 | 25 | 62.5 | 1.5 | 0.075 | 30 | 0.1 | 0 |
| AFC-2 | 225 | 25 | 62.5 | 1.5 | 0.075 | 30 | 0.5 | 0 |
| AFC-3 | 225 | 25 | 62.5 | 1.5 | 0.075 | 30 | 1.0 | 0 |
| AFC-4 | 225 | 25 | 62.5 | 1.5 | 0.075 | 30 | 3.0 | 0 |
| AFC-5 | 225 | 25 | 62.5 | 1.5 | 0.075 | 30 | 0.5 | 1.0 |
| AFC-6 | 225 | 25 | 62.5 | 1.5 | 0.075 | 30 | 0.5 | 2.0 |
| AFC-7 | 225 | 25 | 62.5 | 1.5 | 0.075 | 30 | 0.5 | 3.0 |
| AFC-8 | 225 | 25 | 62.5 | 1.5 | 0.075 | 30 | 0.5 | 4.0 |

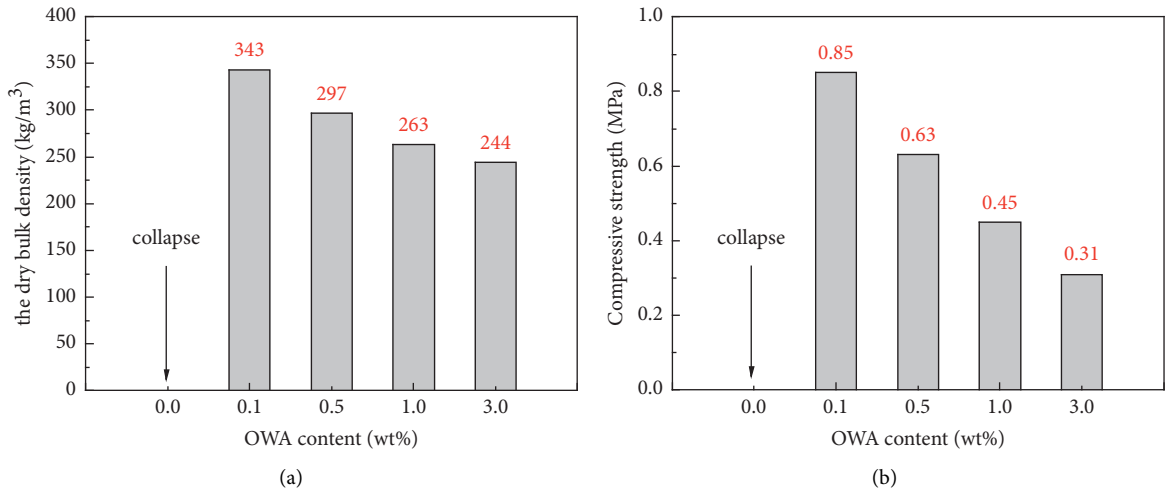


Figure 1: Effect of different OWA content on (a) dry bulk density and (b) compressive strength.

the increasing dosage of OWA from 0.1% to 3.0%, the dry bulk density and compressive strength were significantly decreased. This is because the hydrophobic cement particles adsorb on the gas-liquid interface of the bubble, which could prevent the bubble from further growing and merging [17] and delay the hydration reaction, resulting in reduced compressive strength of specimens [18, 19].

*3.2. Influence of OWA Content on Water Absorption Rate and Thermal Conductivity.* As shown in Figure 2(a), with the increase in OWA content from 0.1% to 3%, the water absorption rate of AFC was significantly decreased from 16.9% to 9.2%. As shown in Figure 2(b), the thermal conductivity of AFC was obviously reduced from 0.104 W/(m·k) to 0.073 W/(m·k). It was seen that with the content of OWA more than 0.5%, the decline tendency of water absorption rate and thermal conductivity became much less obvious. The results indicated that the optimum content of OWA is 0.5% for improving the waterproofing properties of AFC. According to the result of Hai-li [20], the aerogel is effective in enhancing the moisture resistance of foam concrete and forming hydrophobicity on the interfacial substrate of air pores.

When OWA content was kept as 0.5%, the bulk density, compressive strength, water absorption rate, and thermal conductivity of the AFC were 300 kg/m$^3$, 0.6 MPa, 12%, and 0.08 W/(m·k), respectively. The OWA content was kept constant as 0.5% in the following mix proportion.

*3.3. Influence of NSAP Content on Water Absorption Rate and Thermal Conductivity.* Figure 3 presents the influence of NSAP content on water absorption rate and thermal insulation of AFC. It can be seen from Figure 3(a) that with the addition of NSAP from 0% to 4.0%, the water absorption rate first slightly decreased and then significantly increased, reaching a minimum value of 9.2% at 3.0% NSAP. This is because with the increase in the content of small particle NSAP, the consistency and viscosity of foamed concrete slurry increase, resulting in a decrease in the number of connected pores. On the other hand, the microaggregate effect of NSAP reduces the number of capillary pores in the cement paste of foamed concrete [21, 22]. Once when the content of NSAP exceeded 3.0%, the reduction of C-S-H amount in hydration products led to an increase in a number of connected pores. As shown in Figure 3(b), with the increasing content of NSAP from 0% to 4.0%, the thermal conductivity was decreased from 0.074 W/(m·K) to 0.055 W/(m·K). The reasons for the decrease in thermal conductivity are as follows. Firstly, the NSAP with high void fraction decreased the heat transmission route in AFC. Secondly, the thermal conductivity of NSAP is 0.019 W/(m·K), which is lower than the thermal conductivity of air (0.024 W/(m·K)) [23]. Thirdly, concrete materials will become rougher, more loose, and

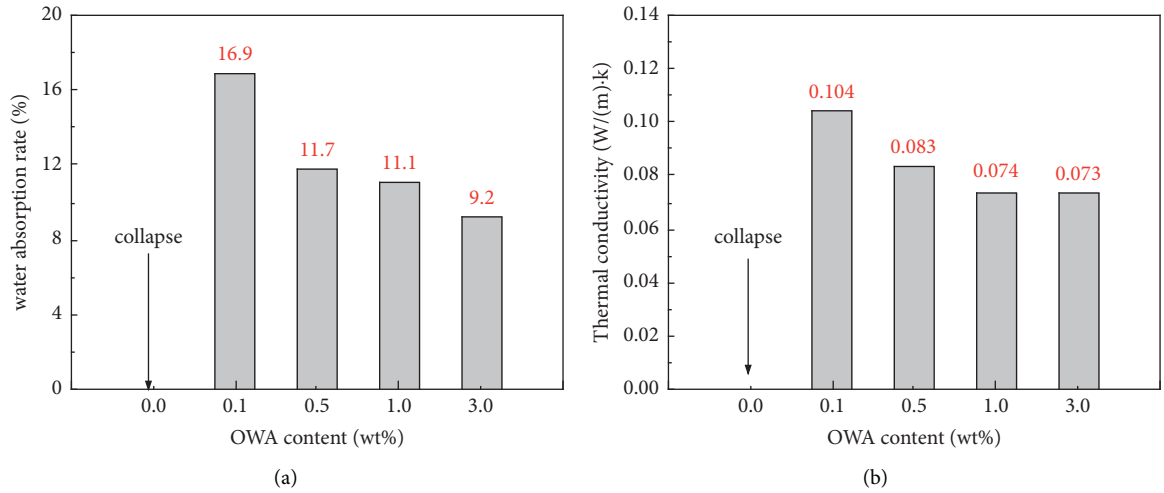


Figure 2: Effect of different OWA content on (a) water absorption rate and (b) thermal conductivity.

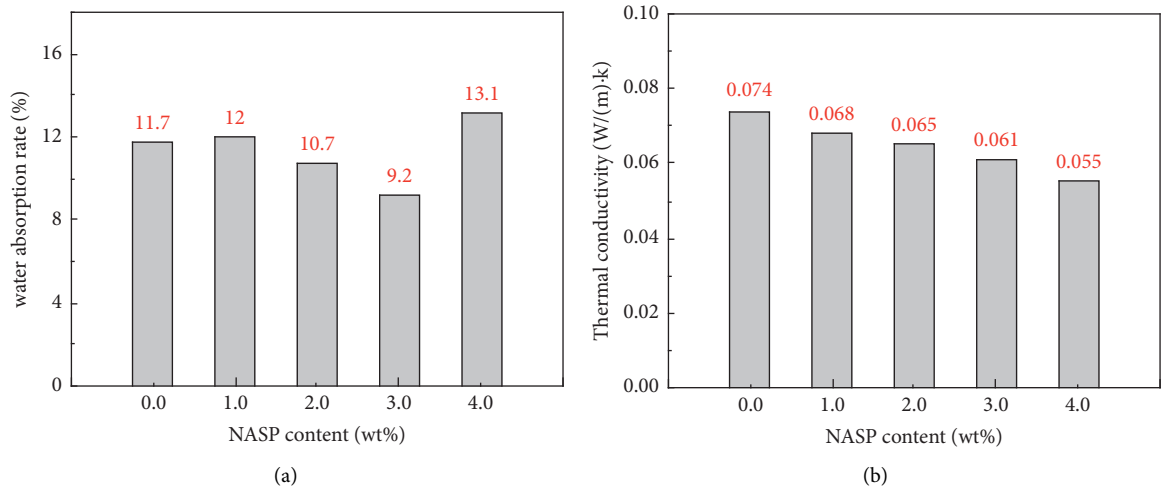


Figure 3: Effect of different NASP content on (a) water absorption rate and (b) thermal conductivity.

porous when NSAP particles are used [24]. Thus, the thermal conductivity was decreased.

## 4. Microstructure and Hydration Products Analysis

*4.1. Pore Structure Analysis.* The microstructure photographs and pore size distribution of AFC-2 and AFC-7 cross section are shown in Figure 4. It was seen that the AFC-2 sample has a small pore size and thick pore wall, while the AFC-7 has a larger average pore size and more macropore amount. It indicated that the addition of NSAP could significantly increase the average pore size and macropore amount of specimens due to the poor combination of NSAP and cement pastes. The results also can explain why the thermal conductivity was decreased [25].

*4.2. XRD.* The X-ray diffraction analysis (Figure 5) proved that the CH (PDF 84-1269) and ettringite (PDF 72-1907) are the main crystalline compounds in all the specimens with or without NSAP. It was also seen that at the peak of 29 degree, C-S-H existed in both AFC-2 and AFC-7. These results indicated that the main hydration products of AFC are CH, C-S-H, and ettringite. Moreover, the addition of NSAP almost had no effect on the hydration products of foamed concrete.

*4.3. SEM.* The SEM images and EDS results of the specimens are shown in Figure 6. As shown in Figures 6(a) and 6(b), the hydration products of AFC-2 and AFC-7 were CH, C-S-H, and ettringite, which further proved the results of XRD. It is seen from Figure 6(b) that there are a large number of NSAP on the surface of AFC hydration product. The EDS results (Figure 7 and the detection position is marked with the red box in Figure 6) of AFC-2 andAFC-7 samples also proved that the particles covering the surface of the hydration product were NSAP. By comparing the SEM images of AFC-2 and AFC-7, it was obvious that the presence of NSAP on the hydration products can weaken the interfacial adhesion between hydration products [26].

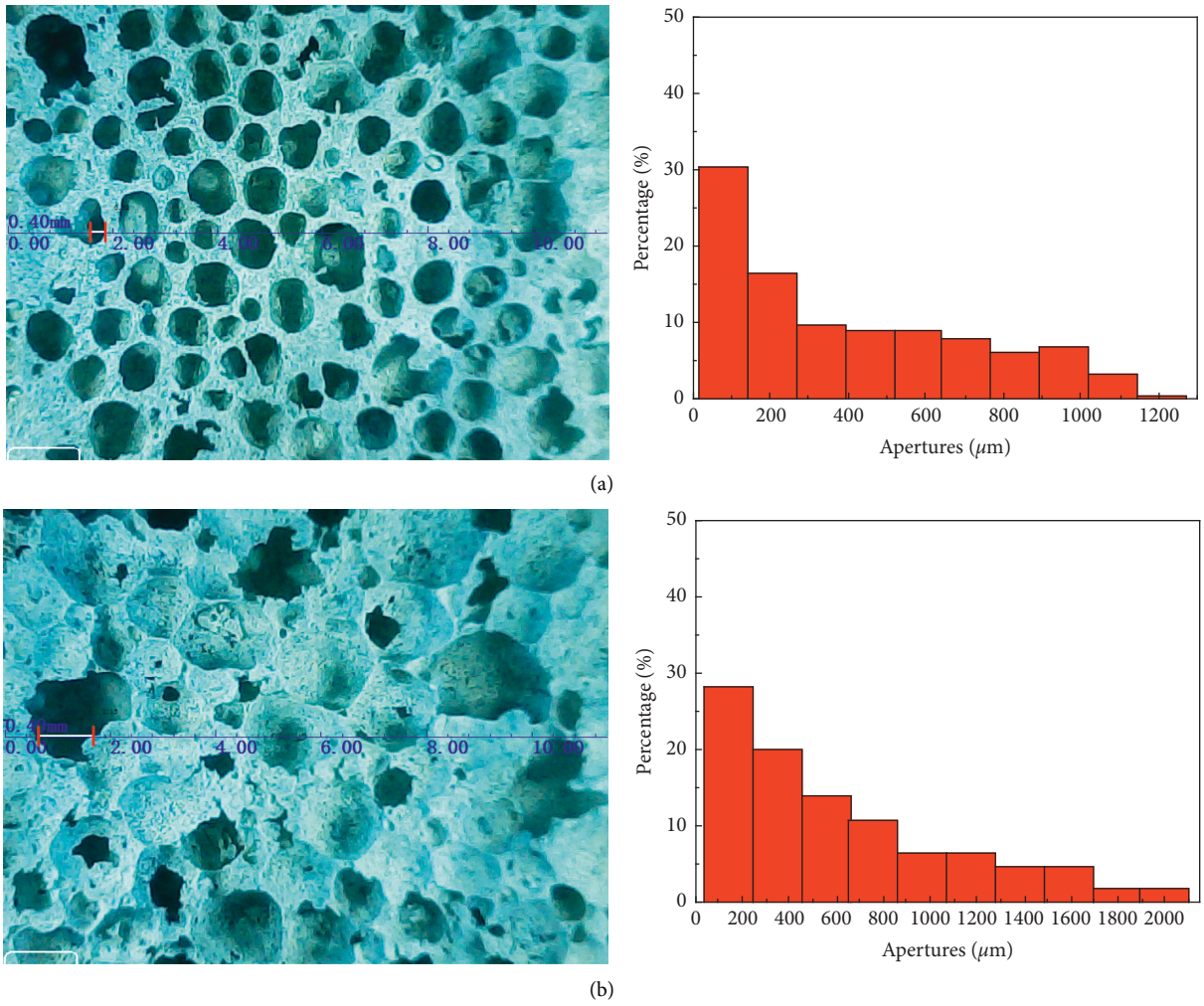


Figure 4: Microstructure photographs and pore size distribution of AFC sample cross section: (a) AFC-2 (without NSAP) and (b) AFC-7 (with NSAP).

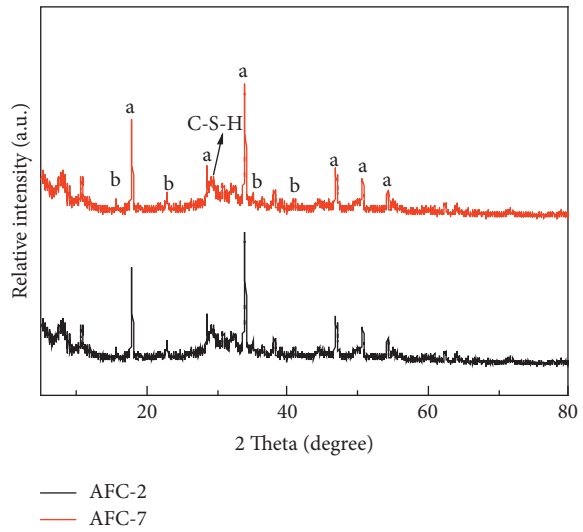


Figure 5: XRD analysis of the hydration products of AFC-7 sample (a for CH; b for ettringite).

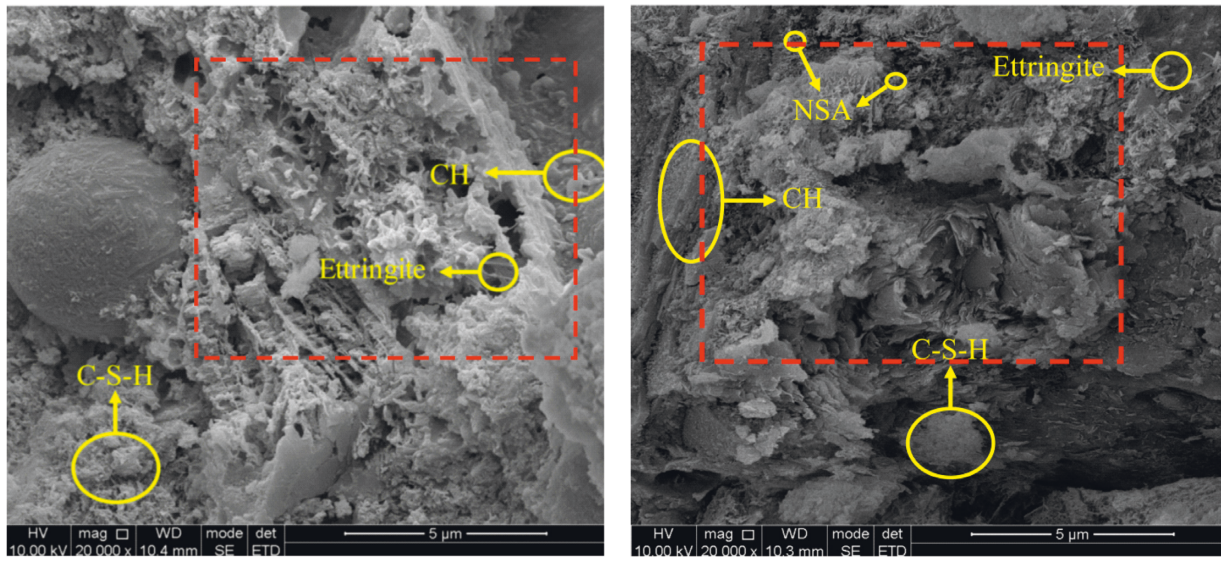


Figure 6: SEM images of (a) AFC-2 (without NSAP) and (b) AFC-7 (with NSAP) sample cross section.

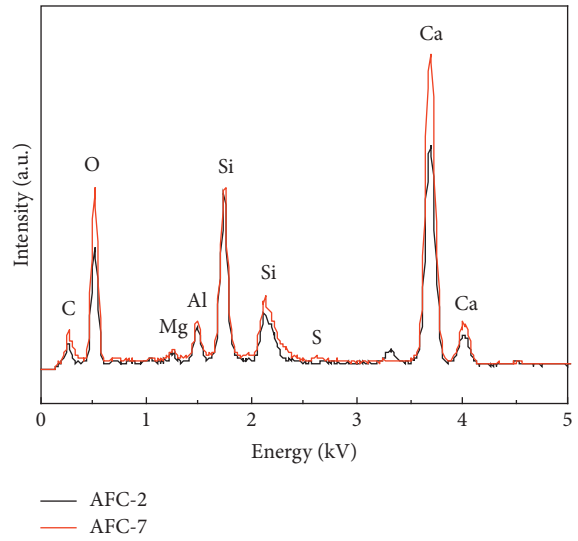


Figure 7: EDS result of AFC-2 and AFC-7 sample.

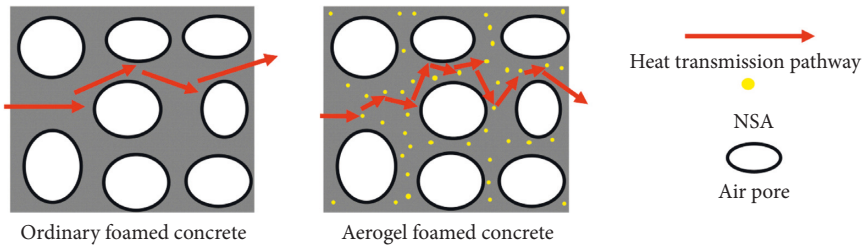


Figure 8: The heat transmission model.

*4.4. Heat Transmission Model.* The heat transmission model of foamed concrete with or without NSAP is presented in Figure 8. It was observed that due to the presence of NSAP, the heat transmission pathway was significantly increased, resulting in more time to complete the heat transfer process [27, 28]. According to equation (1) [29], under the same total heat, material thickness, temperature difference, and heat transmission area, the longer the heat transmission time, the

lower the thermal conductivity. Furthermore, as reported in the literature, the thermal conductivity of gas is much lower than that of solid [28]. When the heat was transferred to the surface of the NSAP, the resistance transmitted through the pores of NSAP increased sharply owing to the NSAP being filled with medium gas. Therefore, the AFC has a lower thermal conductivity compared with ordinary foamed concrete.

$$\lambda = \frac{Qa}{[At(T_2 - T_1)]}, \quad (1)$$

where $\lambda$ is the thermal conductivity, $Q$ is the total heat, $a$ is the material thickness, $A$ is the heat transmission area, $T_2 - T_1$ is the temperature difference, and $t$ is the heat transmission time.

## 5. Conclusion

(1) As OWA content increased, the dry bulk density, compressive strength, water absorption rate, and thermal conductivity of the foamed concrete were decreased. The foam concrete with 3.0% OWA has the best waterproof and thermal insulation performance.

(2) As NSAP content increased, the water absorption rate firstly decreased and then increased while the thermal conductivity was decreased. The AFC with 3.0% NASP not only has low thermal conductivity but also has the lowest water absorption.

(3) The hydration product of AFC was CH, C-S-H, and ettringite. Moreover, the addition of NSAP almost had no effect on the type of hydration product. However, the average pore size and the amount of macropore were significantly increased, and the interfacial adhesion between hydration products was weakened.

(4) In comparison to the heat transmission model, the presence of NSAP could significantly increase the heat transmission pathway and resistance, resulting in the reduction of thermal conductivity.

## Data Availability

The data are generated from experiments and can be available from the corresponding author upon request.

## Conflicts of Interest

The authors declare that they have no conflicts of interest.

## Acknowledgments

This work was supported by National Key Research and Development Plan "Solid Waste Resource" Key Special Project of China (2019YFC1907200), Research and Development Program of CSCEC (CSCEC-2019-Z-24), and Ministry of Housing and Urban Rural Development Research and Development Project (2019-K-049 and 2020-K-173).

## References

[1] Y. H. M. Amran, N. Farzadnia, and A. A. Abang Ali, "Properties and applications of foamed concrete; a review," *Constr. Build. Mater.*vol. 101, pp. 990–1005, 2015.

[2] E. P. Kearsley and P. J. Wainwright, "Porosity and permeability of foamed concrete," *Cement. Concrete. Res.*vol. 31, pp. 805–812, 2001.

[3] F. Roslan, A. Ahmad, M. Hanizam, and M. A. Othuman, "Effects of various additives on drying shrinkage, compressive and flexural strength of lightweight foamed concrete (LFC)," *Adv. Mater. Res.*vol. 626, pp. 594–604, 2012.

[4] W. She, Y. Du, and C. Miao, "Application of organic- and nanoparticle-modified foams in foamed concrete: Reinforcement and stabilization mechanisms," *Cement. Concrete. Res.*vol. 106, pp. 12–22, 2018.

[5] M. R. Jones, K. Ozlutas, and L. Zheng, "Stability and instability of foamed concrete," *Mag. Concrete. Res.*vol. 68, pp. 1–8, 2015.

[6] T. Gao, B. P. Jelle, and A. Gustavsen, "Aerogel-incorporated concrete: An experimental study," *Construction & Building Materials*, vol. 52, no. 2, pp. 130–136, 2014.

[7] H. Jx, G. S. W Hn, and C. Ry, "Study on preparation and properties of intrinsic super-hydrophobic foamed magnesium oxychloride cement material," *Applied Sciences*, vol. 10, no. 8134, pp. 1–15, 2020.

[8] S. Ng, P. B. Jelle, and L. I. C. Sandberg, "Experimental investigations of aerogel-incorporated ultra-high performance concrete," *Construction & Building Materials*, vol. 77, pp. 307–316, 2015.

[9] S. S. Kistler, "Coherent expanded aerogels and jellies," *Nature*, vol. 127, p. 741, 1931.

[10] C. Buratti and E. Moretti, "Glazing systems with silica aerogel for energy savings in buildings," *Appl. Energy.*vol. 98, no. 5, pp. 396–403, 2012.

[11] E. Cuce, P. M. Cuce, C. J. Wood, and S. B. Riffat, "Toward aerogel based thermal superinsulation in buildings: a comprehensive review," *Renew. Sustain. Energy Rev.*vol. 34, no. 3, pp. 273–299, 2014.

[12] K. H. Yang, *Development of high-insulation materials using nano-aerogel and aerated concrete*, Technical report, Kyonggi University, South Korea, 2018.

[13] H. S. Yoon, T. K. Lim, S. M. Jeong, and K. H. Yang, "Thermal transfer and moisture resistances of nano-aerogel-embedded foam concrete," *Construction and Building Materials*, vol. 236, pp. 1–7, 2020.

[14] M. H. Jo, J. K. Hong, and H. H. Park, "Evaluation of $SiO_2$ aerogel thin film with ultra low dielectric constant as an intermetal dielectric," *Microelectron. Eng.*vol. 33, pp. 343–348, 1997.

[15] A. Mccarthy and M. R. Jones, "Preliminary views on the potential of foamed concrete as a structural material," *Mag. Concrete. Res.*vol. 57, pp. 21–31, 2005.

[16] M. A. Othuman Mydin and Y. C. Wang, "Thermal and mechanical properties of lightweight foamed concrete at elevated temperatures," *Mag. Concrete. Res.*vol. 64, pp. 213–224, 2012.

[17] A. Hajimohammadi, T. Ngo, and P. Mendis, "Enhancing the strength of pre-made foams for foam concrete applications," *Cement. Concrete. Comp.*vol. 87, pp. 164–171, 2018.

[18] A. Bagheri and A. Samea, "Effect of air content on rheology of foamed concrete," *Mag. Concrete. Res.*vol. 71, pp. 1–29, 2018.

[19] S. J. Yu, B. Li, and X. L. Chen, "The steel slag fly ash foamed concrete thermal properties [J] Steel Slag Fly Ash Foamed

Concrete Thermal Properties," *Mater. Sci. Froum.*vol. 852, pp. 1398–1403, 2016.

[20] C. Hai-li, "Influence on the performances of foamed concrete by silica aerogels," *Mag. Concrete. Res.*vol. 3, pp. 183–188, 2015.

[21] J. S. Huang, J. Y. Lin, and M. J. Jang, "Stress relaxation of foamed high-alumina cement paste," *Cement . Concrete. Res.*vol. 35, pp. 1503–1509, 2005.

[22] M. Zamin Jumaat, U. Johnson Alengaram, and H. Mahmud, "Shear strength of oil palm shell foamed concrete beams," *Mater. Design.*vol. 30, pp. 2227–2236, 2009.

[23] R. B. Montgomery, "Viscosity and thermal conductivity of air and diffusivity of water vapor in air," *J. Atmos. Sci.*vol. 4, pp. 193–196, 1947.

[24] Q. Zeng, T. Mao, H. D. Li, and Y. Peng, "Thermally insulating lightweight cement-based composites incorporating glass beads and nano-silica aerogels for sustainably energy-saving buildings," *Energy and Buildings*, vol. 174, pp. 97–110, 2018.

[25] H. Y. Sun, A. M. Gong, and Y. L. Peng, "The study of foamed concrete with polypropylene fiber and high volume fly ash," *Appl. Mech. Mater.*vol. 92, pp. 1039–1043, 2011.

[26] S. Wei, Y. Chen, and Y. Zhang, "Characterization and simulation of microstructure and thermal properties of foamed concrete," *Constr. Build. Mater.*vol. 47, pp. 1278–1291, 2013.

[27] M. R. Jones and A. Mccarthy, "Heat of hydration in foamed concrete: Effect of mix constituents and plastic density," *Cement. Concrete. Res.*vol. 36, pp. 1032–1041, 2006.

[28] A. Lamy-Mendes, F. S. Rui, and L. Duraes, "Advances in carbon nanostructure–silica aerogel composites: A review," *J. Mater. Chem. A.Journal of Materials Chemistry A*, vol. 6, pp. 1340–1369, 2018.

[29] E. P. Kearsley, A. S. Tarasov, and H. F. Mostert, "Heat evolution due to cement hydration in foamed concrete," *Mag. Concrete. Res.*vol. 62, pp. 895–906, 2010.